

Early Detection of Liver Steatosis using Multiparametric Ultrasound Imaging

Lokesh Basavarajappa¹, Junjie Li¹, Haowei Tai², Jane Song¹, Kevin J. Parker³, Kenneth Hoyt¹

¹ Department of Bioengineering, University of Texas at Dallas, Richardson, TX, USA

² Department of Electrical and Computer Engineering, University of Texas at Dallas, Richardson, TX, USA

³ Department of Electrical and Computer Engineering, University of Rochester, Rochester, NY, USA

Abstract—Nonalcoholic fatty liver disease (NAFLD) is common and includes a progression from steatosis, nonalcoholic steatohepatitis, to cirrhosis. Liver biopsy is the current standard for detecting the histologic features of NAFLD, but use is limited by invasiveness, sampling error, and potential complications. There is an ongoing need for the ability to noninvasively detect, accurately stage, and reliably monitor NAFLD in the clinical setting. To this end, we recently introduced an *in vivo* multiparametric ultrasound (mpUS) imaging approach to assess NAFLD. Our mpUS integrates contrast-enhanced ultrasound (US), shear wave elastography, and H-scan US measurements. In this paper, we further detail the use of mpUS imaging for the detection of early liver steatosis. Using rats fed either standard control chow ($N = 4$) or a methionine and choline deficient (MCD) diet ($N = 6$) that is known to induce liver steatosis, mpUS imaging was performed at baseline and again at 2 wk. Animals were then humanely euthanized and livers surgically removed for *ex vivo* analysis. Relative changes between baseline and 2 wk were analyzed and only the H-scan US measures in the MCD diet-fed animals were significantly different ($p = 0.03$). Histology confirmed liver steatosis in animals fed the MCD diet.

Keywords—contrast-enhanced ultrasound, fatty liver disease, H-scan ultrasound, shear wave elastography, tissue characterization.

I. INTRODUCTION

Nonalcoholic fatty liver disease (NAFLD) is common and impacts between 80 to 100 million individuals in the United States alone [1]. NAFLD is a disease that includes steatosis, nonalcoholic steatohepatitis (NASH), and cirrhosis, Fig 1. Given the widespread incidence of liver disease, a liver biopsy could be recommended for all NAFLD patients [2]. When detected early, simple lifestyle changes including a healthy diet and exercise can mitigate NAFLD and drastically improve patient prognosis.

Liver biopsy has been the gold standard for assessing hepatocyte injury from NASH. However, liver biopsy is invasive, associated with sampling errors, has higher inter- and intra-rater variability, poor patient acceptance, and potential complications such as bleeding and death leading to poor patient acceptance [3]. Alternatively, considerable effort has been focused on the development of imaging techniques that can help noninvasively detect, accurately stage, and reliably monitor NAFLD. Ideally, findings from these imaging techniques could be used as a biomarker to supplant or minimize the clinical use of invasive liver biopsies.

Reliable methods for NAFLD staging include magnetic resonance elastography (MRE) and magnetic resonance imaging-derived proton density fat fraction (MRI-PDFF). The MRE technique assesses liver stiffness, which is based on an analysis of propagating shear waves that are induced by low frequency vibrations applied to the abdominal wall. Measurements have been shown to correlate with the degree of fibrosis [4]. MRI-PDFF provides a biomarker of steatosis and can be used to accurately estimate liver fat content [5]. Despite strengths, these techniques are not practical for routine clinical screening of early stage NAFLD. Alternatively, ultrasound (US) imaging is evolving as a cost-effective alternative for the early detection of steatosis [6].

Our group recently introduced an *in vivo* multiparametric US (mpUS) imaging technique for the assessment of NAFLD [7]. This mpUS imaging approach integrates contrast-enhanced US (CEUS) to evaluate tissue perfusion, shear wave elastography (SWE) to assess liver viscoelasticity, and H-scan US to investigate the tissue microstructure (i.e., relative scatterer size). Each of these US imaging modes provides complementary information and unique insight into select characteristics of NAFLD. An initial study evaluated the sensitivity of *in vivo* mpUS imaging for monitoring the progression of NAFLD using an established animal model of liver disease [8], [9]. While results from this preliminary proof-of-concept study demonstrated that repeat mpUS measurements could differentiate steatotic from normal livers, *ex vivo* analysis of liver tissue was only performed at termination. In the research presented here, we confirm the repeatability of this previous study's findings, and obtain histology information at an earlier

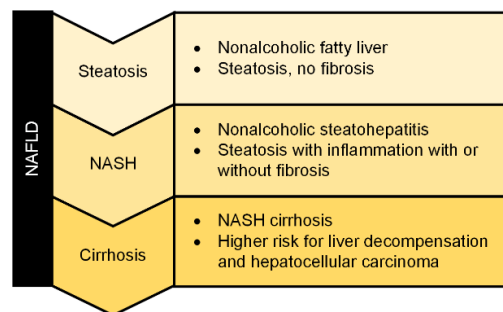


Fig. 1. Stages of nonalcoholic fatty liver disease (NAFLD) including steatosis through hepatocyte injury (inflammation, nonalcoholic steatohepatitis or NASH) and end stage liver cirrhosis.

time point of NAFLD progression to provide a gold standard measure of steatosis.

II. MATERIALS AND METHODS

A. Animal Preparation

Animal experiments were approved by the Institutional Animal Care and Use Committee (IACUC) at the University of Texas at Dallas. A population of Sprague-Dawley rats (Charles River Laboratories, Wilmington, MA) were divided into two groups, namely, control ($N=4$) and diet ($N=6$). Control animals were fed a standard chow while diet animals received a methionine and choline deficient (MCD) chow that is widely known to induce NAFLD.

B. Multiparametric US Imaging

In vivo mpUS imaging of the liver in all animals occurred at baseline (0 wk) and again after 2 wk of feeding. SWE was performed using a Vantage 256 US system (Verasonics Inc, Kirkland, WA) and L11-4v linear array transducer. The SWE pulse sequence consisted of 3 rapid push beams applied using a pulse frequency of 5.2 MHz, aperture size of 64 elements, pulse length of 230 μ s, and axial spacing between push beams of 2 mm. Shear wave propagation was tracked using plane wave imaging (frame rate of 10 kHz). Custom MATLAB software (MathWorks Inc, Natick, MA) was used to calculate tissue displacement from the beamformed in-phase quadrature (IQ) data [10]. A 2-D fast Fourier transform of the tissue displacement data was then used for parametric estimation of liver tissue viscoelasticity, namely, the shear wave speed (SWS) and attenuation (SWA) [11].

H-scan US imaging was performed by a Vevo 3100 system (FUJIFILM VisualSonics Inc, Toronto, Canada) using a MX201 linear array transducer (center frequency of 15 MHz). After attenuation correction [12], beamformed data in radiofrequency (RF) format was collected in the liver and processed using a pair of convolution filters constructed using Gaussian-weighted Hermite polynomial functions of order 2 and 8 (denoted GH_2 and GH_8 , respectively) as described previously [13]–[15]. The relative strength of the filter outputs was normalized by the signal energy $\sqrt{E_n}$. Lower frequency backscattered US signals (GH_2) were assigned to a red (R) channel and higher frequency components (GH_8) to a blue (B) channel. The envelope of the original unfiltered data was assigned to a green (G) channel to complete the RGB color map. H-scan US image intensity was calculated as a ratio of the B channel to the sum of the R and B channels to describe relative scatterer size (RSS) [16].

Lastly, CEUS was also performed using the Vevo 3100 US system but in a MB-sensitive nonlinear imaging mode (center frequency of 12.5 MHz). After receiving a controlled bolus injection of a MB contrast agent via the tail vein (50 μ L; Definity, Lantheus Medical Imaging, N Billerica, MA), CEUS images were acquired (approximately 1 min of data). After placement of a region-of-interest (ROI) in the liver parenchyma and a second one circumscribing the inferior vena cava (IVC), mean time-intensity curves were calculated. From each of these temporal curves, peak enhancement (PE) and wash-in rate (WIR) parameters were derived, representing surrogate measures of blood volume and flow rate, respectively [17], [18].

CEUS parameters from the liver were normalized by those from the IVC. Note CEUS imaging was performed last in the mpUS sequence because any residual MBs in circulation could induce bioeffects if exposed to US intensities used for SWE [19].

C. Histological Analysis

Animals were euthanized after 2 wk of *in vivo* mpUS imaging. Each liver was surgically removed for *ex vivo* analysis. Liver tissue was embedded in paraffin, sectioned, and stained with hematoxylin and eosin (H&E) or Picrosirius red. High-resolution optical images for each tissue section were acquired using an inverted fluorescence microscope (Axio Observer 7, Carl Zeiss, Thornwood, NY) used for steatosis and fibrosis detection. H&E images were binarized and processed with morphological operations before quantification of liver steatosis as a percent fat fraction.

D. Performance Measures

Data was summarized as mean \pm standard deviation. A Mann-Whitney or Wilcoxon matched pairs signed rank test was used to assess the *in vivo* or *ex vivo* control and diet group data. A p -value less than 0.05 was statistically significant. All statistical tests were performed using Prism 9 (GraphPad Software Inc, San Diego, CA).

III. RESULTS

Multiparametric US imaging was performed using animals fed a standard chow or MCD diet at baseline and again at 2 wk. The mpUS approach included *in vivo* measures of SWS and SWA from SWE, RSS from H-scan US, and PE and WIR from CEUS. Figure 2 summarizes the progression of these US-derived parametric estimates in rat liver. Comparing data from animals fed the MCD to controls, SWE measurements indicate that the SWS parameter from the liver parenchyma was reduced by 20% (control, 1.5 ± 0.3 m/s; diet, 1.2 ± 0.1 m/s) and the SWA parameter increased by 18.4% (control, 91.8 ± 6.6 Np/m; diet, 112.5 ± 25.7 Np/m). Correspondingly, RSS values from use of H-scan US imaging increased by 22.5% (control, 54.7 ± 2.6 ; diet, 67.2 ± 3.4) and the CEUS imaging-derived PE parameter increased by 36.4% (control, 1.1 ± 0.5 ; diet, 1.5 ± 1.0) and the WIR parameter by 25% (control: 0.4 ± 0.3 , Diet: 0.5 ± 0.5). Relative changes between baseline and 2 wk were analyzed and only the H-scan US measures in the MCD diet fed animals were found to be statistically different ($p = 0.03$), although SWS measures trended towards significance ($p = 0.09$).

It is worth noting that while control animals grew and gained weight throughout this short 2 wk study, animals fed the MCD diet actually lost some weight and were smaller at termination ($p = 0.01$). After euthanasia at 2 wk, livers were excised for *ex vivo* analysis. A comparison of liver weights from control and MCD diet fed animals at termination revealed the latter were significantly lighter ($p = 0.005$). These liver tissues underwent histological processing to assess the presence of liver steatosis and fibrosis from the H&E and Picrosirius red stained tissue sections, respectively. Inspection of the representative histology images presented in Figure 3 reveals that the animal fed the MCD diet exhibited considerable liver steatosis not found in the control animal. Liver fibrosis in both was minimal. These

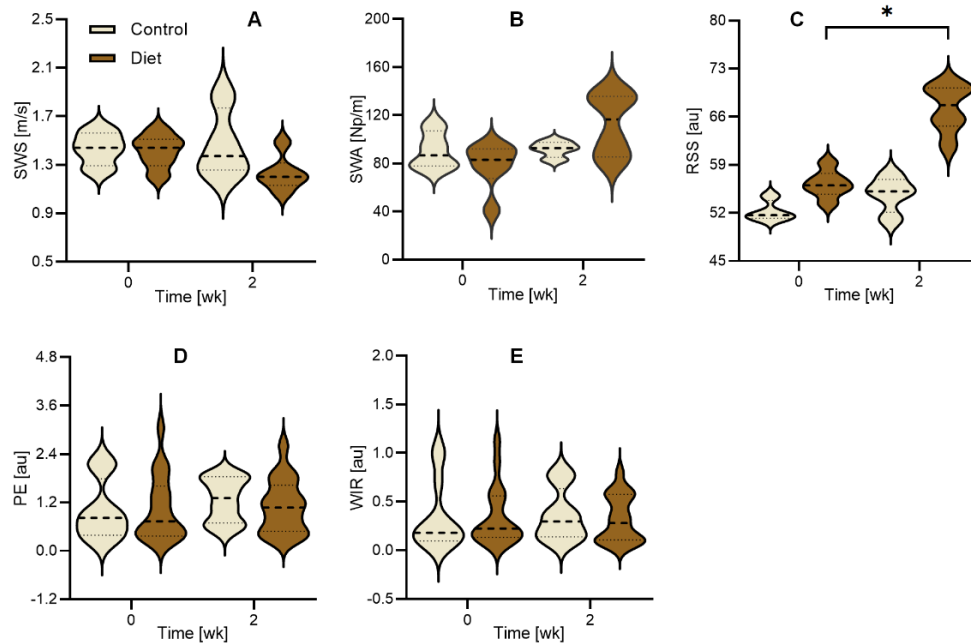


Fig. 2. Summary of *in vivo* multiparametric ultrasound (mpUS) liver measurements from rats fed standard chow or a diet that induces NAFLD. Shown are plots for the following mpUS parameters taken from the liver parenchyma: (A) shear wave speed (SWS), (B) shear wave attenuation (SWA), (C) relative scatterer size (RSS), (D) peak enhancement (PE), and (E) wash-in rate (WIR). * denotes $p < 0.05$ relative to baseline.

patterns were consistent in all histology sections. H&E images were binarized to locate fat deposits and a fat fraction score was calculated. Longitudinal changes in the fat fraction are summarized in Figure 4. The mean fat fraction value from the MCD diet and control group animals were $19.6 \pm 4.1\%$ and $0.3 \pm 0.1\%$, respectively ($p = 0.01$).

IV. DISCUSSION

The *in vivo* mpUS imaging approach used for this preclinical study integrated SWE parameters to access liver viscoelasticity, CEUS for blood flow, and H-scan US to obtain information on the liver tissue microstructure. Preliminary findings suggest that mpUS imaging can provide a comprehensive estimation of the main features of early stage NAFLD. A previous study detailed the progression of mpUS parameters in rat livers at 0 (baseline), 2, and 6 wk after animals were placed on a standard chow or

MCD diet [8]. Interestingly, substantial changes in the mpUS parameters were found between the control and diet group animals at 2 wk. However, that study design did not include histological analyses to compare to the *in vivo* mpUS findings. This was the impetus to confirm the early stage results with the addition of termination and *ex vivo* analysis of liver tissue samples at the earlier time point (2 wk). It was hypothesized that these early histology results might provide additional insight into the sensitivity of mpUS imaging to early NAFLD progression.

Preclinical mpUS results detailed herein were consistent with previous studies [7]–[9]. More specifically, it was shown

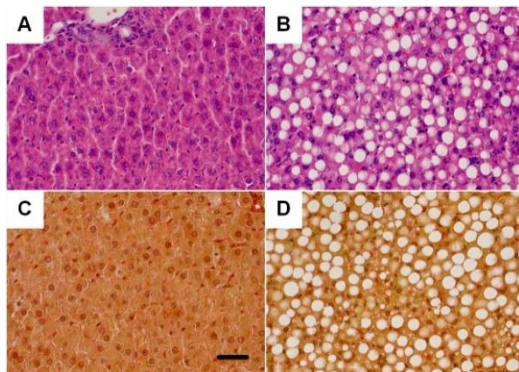


Fig. 3. Histology images of (A, B) hematoxylin and eosin (H&E) and (C, D) Picrosirius red stained liver tissue sections from an animal fed (A, C) standard chow (control) or a (B, D) diet that induces NAFLD for 2 wk. Note the high level of steatosis (white circular voids) in the diet fed animal liver.

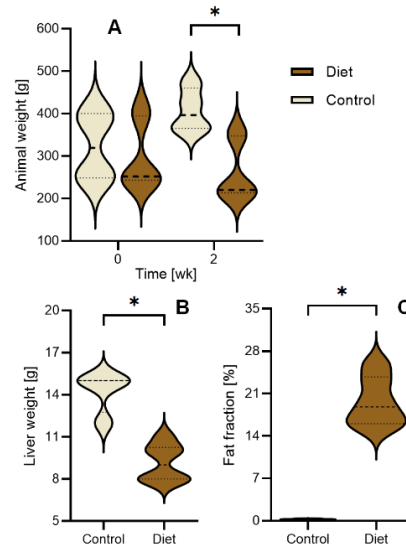


Fig. 4. Summary of (A) changes in animal weight, (B) excised liver weight, and the (C) fat fraction score derived from histology measurements.

that changes in the H-scan US format for characterizing RSS were most significant after initiating an NAFLD-inducing diet compared to the other mpUS parameters. The potential explanation for these changes may be that the onset of liver steatosis increases the mean distance between hepatocytes and the effective US scatterers [20], and that the accumulation of small fat vacuoles adds a Rayleigh component to the backscattered US signals from background liver structures [9].

Given that animals with NAFLD only developed simple liver steatosis, it could be intimated that disease progression to different stages of NASH and fibrosis would progressively impact other mpUS parameters. For example, it has been shown that the onset of liver fibrosis results in a marked increase in the SWS parameter during a SWE examination [21]. To observe these progressive changes in liver in the preclinical setting, the MCD diet may not be sufficient and a different animal model of NAFLD may be needed. Future work will further examine mpUS parameters and compare to more established noninvasive imaging techniques such as MRI-PDF.

V. CONCLUSIONS

This preclinical study further evaluated the use of *in vivo* mpUS measurements for the detection of NAFLD. When liver steatosis was the only dominant feature as confirmed by *ex vivo* analysis of liver tissue samples, RSS estimates using H-scan US imaging were the most sensitive to early changes.

ACKNOWLEDGEMENTS

This research was supported by National Institutes of Health (NIH) grants R01DK126833 and R21EB025290, and award RP180670 from the Cancer Prevention and Research Institute of Texas (CPRIT) to establish the Small Animal Imaging Facility at the University of Texas at Dallas.

REFERENCES

- [1] J. D. Browning *et al.*, "Prevalence of hepatic steatosis in an urban population in the United States: impact of ethnicity," *Hepatology*, vol. 40, no. 6, pp. 1387–1395, 2004.
- [2] J. K. J. Gaidos, B. E. Hillner, and A. J. Sanyal, "A decision analysis study of the value of a liver biopsy in nonalcoholic steatohepatitis," *Liver Int*, vol. 28, no. 5, pp. 650–658, 2008.
- [3] D. E. Kleiner *et al.*, "Design and validation of a histological scoring system for nonalcoholic fatty liver disease," *Hepatology*, vol. 41, no. 6, pp. 1313–1321, 2005.
- [4] S. Jayakumar *et al.*, "Longitudinal correlations between MRE, MRI-PDF, and liver histology in patients with non-alcoholic steatohepatitis: Analysis of data from a phase II trial of selonsertib," *J Hepatol*, vol. 70, no. 1, pp. 133–141, 2019.
- [5] B. Wildman-Tobriner *et al.*, "Association between magnetic resonance imaging-proton density fat fraction and liver histology features in patients with nonalcoholic fatty liver disease or nonalcoholic steatohepatitis," *Gastroenterology*, vol. 155, no. 5, pp. 1428–1435, 2018.
- [6] A. Ozturk *et al.*, "Quantitative hepatic fat quantification in non-alcoholic fatty liver disease using ultrasound-based techniques: A review of literature and their diagnostic performance," *Ultrasound Med Biol*, vol. 44, no. 12, pp. 2461–2475, 2018.
- [7] L. Basavarajappa *et al.*, "Early assessment of nonalcoholic fatty liver disease using multiparametric ultrasound imaging," *Proc IEEE Ultrason Symp*, pp. 1–4, 2020.
- [8] L. Basavarajappa *et al.*, "Multiparametric ultrasound imaging for the assessment of normal versus steatotic livers," *Sci Rep*, vol. 11, no. 1, p. 2655, 2021.
- [9] J. Baek *et al.*, "Clusters of ultrasound scattering parameters for the classification of steatotic and normal livers," *Ultrasound Med Biol*, 2021.
- [10] T. Loupas, R. B. Peterson, and R. W. Gill, "Experimental evaluation of velocity and power estimation for ultrasound blood flow imaging, by means of a two-dimensional autocorrelation approach," *IEEE Transactions on Ultrasonics, Ferroelectrics, and Frequency Control*, vol. 42, no. 4, pp. 689–699, 1995.
- [11] I. Z. Nenadic *et al.*, "Attenuation measuring ultrasound shearwave elastography and *in vivo* application in post-transplant liver patients," *Phys Med Biol*, vol. 62, no. 2, pp. 484–500, 2017.
- [12] H. Tai, M. Khairalseed, and K. Hoyt, "Adaptive attenuation correction during H-scan ultrasound imaging using K-means clustering," *Ultrasonics*, vol. 102, p. 105987, 2020.
- [13] M. Khairalseed, K. Brown, K. J. Parker, and K. Hoyt, "Real-time H-scan ultrasound imaging using a Verasonics research scanner," *Ultrasonics*, vol. 94, pp. 28–36, 2019.
- [14] M. Khairalseed, F. Xiong, J.-W. Kim, R. F. Mattrey, K. J. Parker, and K. Hoyt, "Spatial angular compounding technique for H-scan ultrasound imaging," *Ultrasound Med Biol*, vol. 44, no. 1, pp. 267–277, 2018.
- [15] M. Khairalseed, K. Javed, G. Jashkaran, J.-W. Kim, K. J. Parker, and K. Hoyt, "Monitoring early breast cancer response to neoadjuvant therapy using H-scan ultrasound imaging: Preliminary preclinical results," *J Ultrasound Med*, vol. 38, no. 5, pp. 1259–1268, 2019.
- [16] M. Khairalseed, K. Hoyt, J. Ormachea, A. Terrazas, and K. J. Parker, "H-scan sensitivity to scattering size," *J Med Imaging*, vol. 4, no. 4, p. 043501, 2017.
- [17] R. Saini and K. Hoyt, "Recent developments in dynamic contrast-enhanced ultrasound imaging of tumor angiogenesis," *Imaging Med*, vol. 6, no. 1, pp. 41–52, 2014.
- [18] K. Hoyt, H. Umphrey, M. Lockhart, M. Robbin, and A. Forero-Torres, "Ultrasound imaging of breast tumor perfusion and neovascular morphology," *Ultrasound Med Biol*, vol. 41, no. 9, pp. 2292–2302, 2015.
- [19] A. G. Sorace, J. M. Warram, H. Umphrey, and K. Hoyt, "Microbubble-mediated ultrasonic techniques for improved chemotherapeutic delivery in cancer," *J Drug Target*, vol. 20, no. 1, pp. 43–54, 2012.
- [20] M. Khairalseed, G. Rijal, and K. Hoyt, "Spatial comparison between the H-scan format for classification of ultrasound scatterers and histology - Preliminary results using an animal model of breast cancer," *Proc IEEE Ultrason Symp*, pp. 1–4, 2020.
- [21] S. S. Poul and K. J. Parker, "Fat and fibrosis as confounding cofactors in viscoelastic measurements of the liver," *Phys Med Biol*, vol. 66, no. 4, p. 045024, 2021.